Bio-Enabled Platform to Access Polyamides with Built-In Target Properties

Prerana Carter,[†,‡] James L. Trettin,[†] Ting-Han Lee,[†] Nickolas L. Chalgren,[†] Michael J. Forrester,[†] Brent H. Shanks,[†,‡,*] Jean-Philippe Tessonnier,[†,‡,*] and Eric W. Cochran[†,*]

[†]Department of Chemical and Biological Engineering, Iowa State University, Ames, Iowa 50011, United States

[‡]Center for Biorenewable Chemicals (CBiRC), Ames, Iowa 50011, United States

*E-mail: bshanks@iastate.edu, tesso@iastate.edu, ecochran@iastate.edu

KEYWORDS: muconic acid, Diels-Alder cycloaddition, polyamides, hydrophobic, flame-retardant, biobased molecules

ABSTRACT: The diversification of platform chemicals is key to today's petroleum industry. Likewise, the flourishing of tomorrow's biorefineries will rely on molecules with next-generation properties from biomass. Herein, we explore this opportunity with a novel approach to monomers with custom property enhancements. Cyclic diacids with alkyl and aromatic decorations were synthesized from muconic acid by Diels-Alder cycloaddition, and copolymerized with hexamethylenediamine and adipic acid to yield polyamides with built-in hydrophobicity and flame retardancy. Testing shows a 70% reduction in water uptake and doubling of char production while largely retaining other key properties of the parent Nylon-6,6. The present approach can be generalized to access a wide range of performance-advantaged polyamides.

The polymer industry is a key driver in the transition to biomass as a carbon feedstock,[1,2] having bolstered the production of bioreplacements for adipic acid, acrylonitrile, and methacrylic acid, among others.[3,4] Moreover, it stimulates the discovery of novel molecules and functionalities that could rejuvenate the biochemical industry.[5,6] For example, the polyesterification of 2,5-furandicarboxylic acid (FDCA) to polyethylene furanoate (PEF) yields a bioplastic with superior mechanical, thermal, and barrier properties compared to polyethylene terephthalate (PET).[7] However, biopolymer discovery typically follows a pipeline approach beginning with a biobased platform intermediate and conversion to a single targeted monomer that is further (co)polymerized.[8–10] The cost and effort associated with this approach are considerable, and represent significant risk because *a priori* polymer property prediction remains elusive.[11]

Here, we demonstrate a streamlined process to accelerate the discovery of performance-advantaged biomonomers. By embracing biobased platform chemicals, in particular bioprivileged muconic acid (MA), properties in conventional polymers like polyamide-6,6 (Nylon-6,6) can be tailored without significant trade-offs.[12,13]

Produced fermentatively from lignocelluosic feedstocks,[14] biopriveledged MA is an attractive candidate as a starting molecule for diversity-oriented syntheses[15] to drop-in monomer replacements such as adipic acid (AA),[16,17] terephthalic acid (TPA),[18–20] ε-caprolactam,[21,22] and hexamethylene diamine[23]; additionally, novel species like 3-hexenedioic acid and cyclohex-1/2-ene dicaboxylic acid have been reported.[24–26] Work to upgrade MA to TPA and cyclohexane-1,4-dicarboxylic acid (CH1DA) showed that *trans,trans*-MA (*tt*MA) would undergo Diels-Alder cycloaddition (DA) as a diene using ethylene as the dieneophile.[27,28] Evidently, steric effects render *tt*MA as the only isomer capable of this reaction. In this work, *tt*MA's conjugated unsaturation is leveraged with DA chemistry to create a family of biobased cyclic diacids. By choosing dieneophiles to imbue desired properties like hydrophobicity or flame retardancy, a variety of performance-enhanced Nylon-6,6 copolymers can be generated (Figure 1).

Hydrophobic diacids were produced through DA with bulky nonpolar α-olefins. There was limited reactivity directly with *tt*MA. However, DA cycloaddition of dimethyl-*trans,trans*-muconate (dm*tt*M), and 1-octene (OC) or 1-tetradecene (TD) readily afforded the cycloadducts with alkyl-pendants of 6-carbons and 12-carbons, respectively (Scheme S1, Figures S1 and S2, Table S1). Base-catalyzed hydrolysis yielded the diacids (Figure 2). ^{1}H nuclear magnetic resonance (NMR) showed aliphatic peaks at 0.8 and 1.2 ppm with integrations near the expected values (Table S2). To test end-use properties, the diacids were independently precipitated as Nylon salts with hexamethylene diamine (HMDA), mixed with AA/HMDA salts, and reacted to form Nylon-6,6 copolymers.[29] A 25 mol% replacement of AA/HMDA salt was tested to observe a prominent effect on

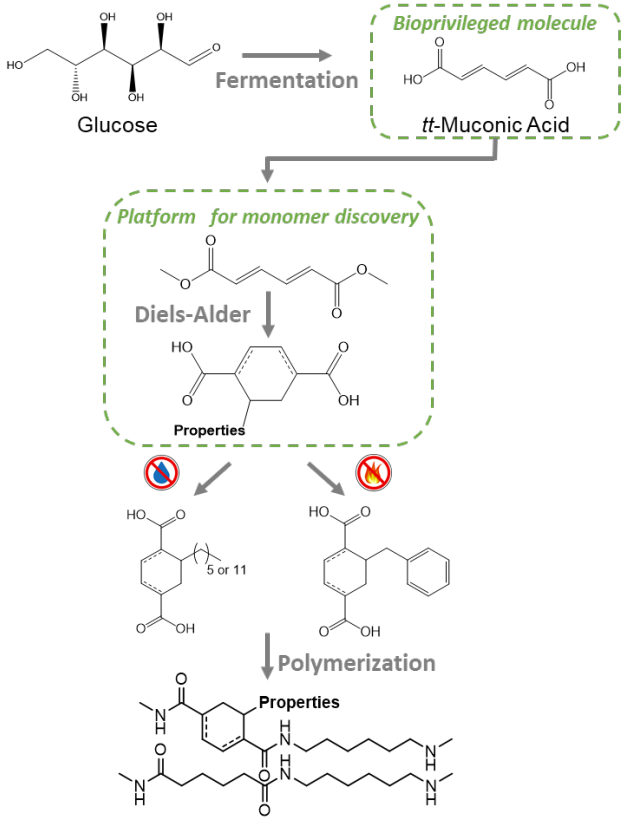

Figure 1. Platform approach for the discovery of property-advantaged comonomers. Bioprivileged *tt*MA is derivatized via Diels-Alder cycloaddition to novel comonomers that enable polyamides with built-in target properties, such as hydrophobicity and flame retardancy.

Nylon-6,6 end-use properties. The polyamides were produced in two stages using a pressurized reactor vessel with continuous agitation. Elemental analysis and ^{1}H NMR confirmed the stability of the novel diacids throughout polymerization (Table S3, Figures S3 and S4). Neat Nylon-6,6 served as a benchmark to these cycloaliphatic polyamides as they were characterized for various properties (Table 1). Under similar polymerization conditions, it was observed that Nylon-6,6 exhibited the highest molecular weight with a dispersity (Đ) of 2, typical of step-growth polymerization.

The cycloaliphatic polyamides showed a decrease in M_n, most notably in CH1DA-OC and CH1DA-TD, which also showed significantly higher Đ values. We primarily attribute these molecular weight distribution (MWD) effects to the wide range in melting points of the various Nylon salts (Table S3) that would promote disparate polymerization rates, particularly during polyamidation start-up. Additionally, the asymmetry of the novel monomers may cause differences in propagation rates. The potential for heterogeneity in CH1DA-OC and TD was investigated through transmission electron microscopy of osmium-stained slices, imparting contrast to the unsaturated bonds (Figure S5). The homogeneity of the micrographs indicates a lack of microphase separation. Future optimization of the polyamidation process will further improve the MWD; here, our purpose is to

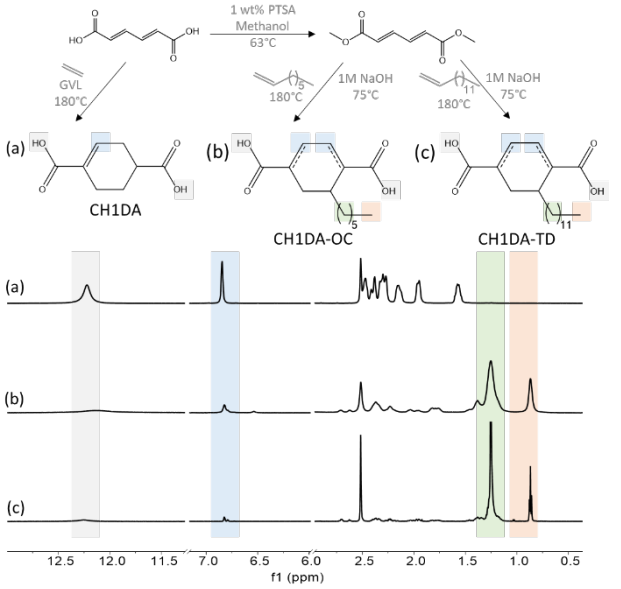

Figure 2. Novel diacid syntheses: direct DA of ttMA and ethylene yields CH1DA, whereas CH1DA-OC and CH1DA-TD were formed by reacting dm*tt*M with the corresponding *α*-olefins. ^{1}H NMR in dimethyl sulfoxide-d_6 confirms the formation of the desired products.

investigate value-added property enhancement imparted by the biobased diacids.

The thermal and crystal behaviors of this family of cycloaliphatic polyamides were characterized through differential scanning calorimetry (DSC), wide-angle X-ray scattering (WAXS), and thermogravimetric analysis (TGA) (Figures S6-S9). DSC showed pure Nylon-6,6 having the highest melting temperature (T_m) and degree of crystallinity (χ_C). The cyclic counits disrupt chain regularity and hydrogen bonding, reducing both T_m and χ_C. For example, CH1DA shows T_m depression of 16 °C and reduction in χ_C by about 30% compared to Nylon-6,6. The long alkyl chains and high dispersity of CH1DA-OC and CH1DA-TD further restricted crystal formation with T_m depression of ≈ 30 °C and χ_C reduction of 54%. TGA under nitrogen showed that the degradation temperature (T_{d10}) increased slightly for all copolymers (Table 1). Pure Nylon-6,6 demonstrated a char yield of 2.9% at 500 °C. It was expected that the hydrocarbon-rich, alkyl-chain functionalized polyamides (CH1DA-OC/TD) would show a lower char yield, which was confirmed experimentally. Insights into the crystal structure were determined through room-temperature WAXS. The semicrystalline nature of the polyamides was confirmed by sharp Bragg peaks representing the crystalline segments and a broad halo characteristic of the amorphous regions. The percent crystallinity (χ_{C_WAXS}) was calculated from the ratio between areas under the peaks normalized over the total area. Nylon-6,6 exhibited two prominent peaks at approximately 20° and 24°, corresponding to the (100) and (010)/(110) doublet of the α-phase.[30] CH1DA and CH1DA-OC showed one broad peak for intrasheet scattering at around 21° whereas CH1DA-TD showed a small shoulder for the scattering of the (010)/(110) plane. This shoulder could be attributed to ordered domains formed by the longer alkyl pendant groups. The similarity among

Table 1. Properties of Nylon-6,6 and novel cycloaliphatic copolyamides at 25 mol% comonomer loading.

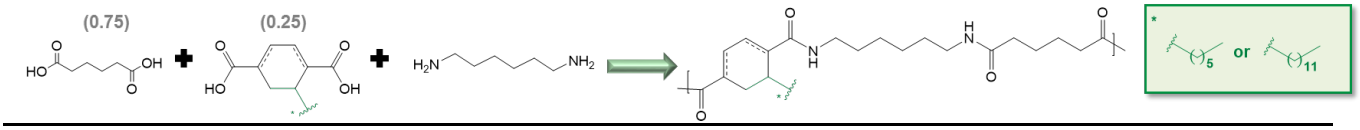

Sample	M_n[a] (kDa)	Đ[a]	T_m[b] [°C]	ΔH_m[b] [J/g]	T_c[b] [°C]	χ_{C_DSC}[b] [%]	T_{g_DSC}[c] [°C]	χ_{C_WAXS}[d] [%]	$Char_{500°C}$[e] [%]	T_{d10}[e] [°C]
Nylon-6,6	34.3	2.0	262.2	67.2	231.4	26.3	72.7	41.5	2.9	410.8
CH1DA	21.6	1.9	245.9	46.2	209.7	18.1	88.1	39.3	3.4	418.7
CH1DA-OC	12.4	4.9	228.1	29.9	177.7	11.7	81.4	37.2	2.4	418.7
CH1DA-TD	15.5	5.2	231.6	30.6	190.6	12.0	76.6	27.0	2.4	418.7

[a] M_n: Number-average molecular weight; Đ: Dispersity from GPC; [b] T_m: Melting temperature; ΔH_m: Enthalpy of melting; T_c: Crystallization temperature; χ_{c_DSC}: Percent crystallinity (DSC); [c] T_{g_DSC}: Glass-transition temperature from modulated DSC and [d] χ_{c_WAXS}: Percent crystallinity from WAXS (annealed); [e] $Char_{500°C}$: Residual mass at 500 °C; T_{d10}: Decomposition temperature at 10% mass loss under N_2 from TGA.

WAXS patterns suggests that the crystalline phase is comprised solely of Nylon-6,6 units with the relegation of cycloaliphatic counits to the amorphous phase.[31] Due to annealing, χ_{C_WAXS} values are 60–220% larger than χ_{C_DSC}. Moreover, only CH1DA-TD shows a marked diminishment in crystallinity from Nylon-6,6. These observations reveal that the crystallization rate is lower in the copolymers.

The novel counits were intended to reduce hygroscopicity, a major drawback of Nylon-6,6. Nylon-6,6 has several hydrophilic amide linkages that attract water, especially in the amorphous domain. Water strongly plasticizes, reduces glass transition temperature (T_g), modulus, and strength while increasing extensibility. Water absorption depends on composition, crystallinity, molding, geometry, and exposure conditions.[32] We characterized hydrophobicity through 24 h water absorption (ASTM D 570), moisture uptake at 50% relative humidity (RH), and contact angle measurements (Figure 3). Samples were injection-molded into the ISO 527-2-1BB geometry prior to testing. Immersion tests showed Nylon-6,6 demonstrated the highest water absorption. This was reduced by 40% in CH1DA-OC, whereas CH1DA-TD had a water uptake of only 0.8%, a 70% decrease from Nylon-6,6. This dramatic reduction is especially significant considering the broad dispersity and reduced crystallinity of the OC/TD samples that counteract the hydrophobicity of the novel monomers. Similar improvements in hydrophobicity are known in castor oil-derived Nylon-6,10 (60% reduction) or Nylon-6,12 (80%).[33,34] However, higher carbon-numbered Nylons differ from Nylon-6,6 in most respects with 100% replacement of adipic acid, with significant compromises in thermal and mechanical properties. Here, the OC/TD copolymers retain many Nylon-6,6 characteristics, including similar T_g values and crystal structure. The polymers at 50% RH followed a similar trend. CH1DA-TD showed the most prominent improvement exhibiting a moisture absorption of only 0.35%. Surface wettability was determined using contact angles, where a higher angle corresponds to a decreased affinity towards water at the solid-liquid interface. Equal surface roughness was ensured prior to testing, to reduce its influence on the observed results. Nylon-6,6 exhibited a contact angle value of ~75°, while CH1DA-OC and CH1DA-TD showed similar performance (~87°).

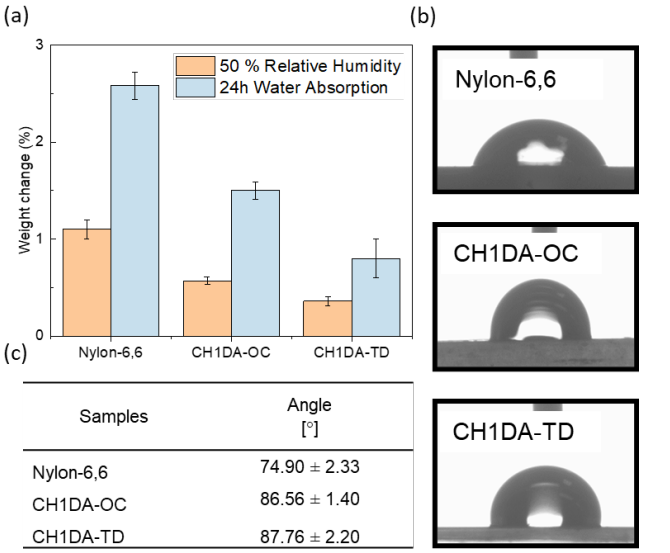

Figure 3. (a) Weight change on 24 h water immersion and 50% RH conditioning for Nylon-6,6, CH1DA-OC and CH1DA-TC. (b) Contact angle images. (c) Contact angle values.

The viscoelastic properties were tested using dynamic mechanical analysis (Figure 4, Table 2). The storage moduli (E') are reported in Table 2 from within the glassy plateau at 0 °C. All cycloaliphatic polyamides showed an increased E' compared to Nylon due to the rigidity introduced by cyclic units in the polymer backbone. While this intimates that the tensile modulus may also be significantly higher, the molecular weight disparity between the novel copoylmers and Nylon-6,6 preclude a thorough direct comparison of mechanical properties until the MWD has been better optimized. T_g for the polymer samples was located at the maxima of tan δ, which corresponds to the ratio between E' and the loss modulus (E"). T_g is strongly influenced by the flexibility and molecular mobility of the polymer backbone and their pendant groups. Additionally, T_g is suppressed by high Đ values, where the proliferation of

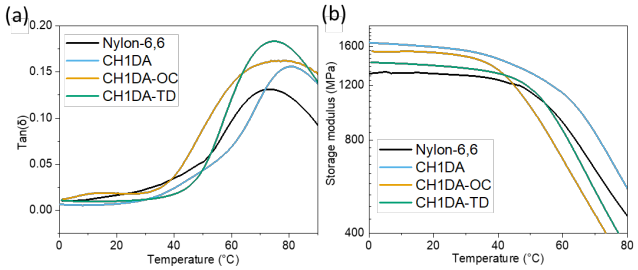

Figure 4. (a) Tan (δ) and (b) storage moduli for dry annealed polyamide series at 10 rad s^{-1} versus temperature at 5 K/min ramp rate.

Table 2. Torsional DMA results of polyamides showing storage moduli, loss moduli, and glass transition temperatures.

Sample	E'[a] [GPa]	E''[a] [MPa]	T_{g_DMA}[b] [°C]	E'$_{sat}$[c] [GPa]	T_{g_sat}[c] [°C]
Nylon-6,6	1.32	16.5	73.3	0.687	-6.5
CH1DA	1.65	10.9	80.3	0.027	1.6
CH1DA-OC	1.55	18.6	78.6	1.06	12.6
CH1DA-TD	1.42	15.6	74.8	0.95	20.9

[a]E' and E'' correspond to storage and loss modulus, respectively, for dry samples at 0 °C. [b]T_g from peak tan (δ). [c]E'$_{sat}$ and T_{g_sat} are the E' and T_g measured after 40 days of water immersion.

smaller chains have a plasticizing effect. The unfunctionalized cycloaliphatic polyamide (CH1DA) had higher E' and T_g than Nylon-6,6 due to the reduced flexibility introduced by the cyclic counits. With the introduction of alkyl pendant groups (CH1DA-OC and CH1DA-TD), two opposing effects could occur. On one hand, chain mobility is restricted due to steric hindrance causing a rise in T_g, whereas an opposing chain-length dependent plasticizing behavior (and dispersity) is expected to decrease T_g.[35] The latter effects dominate, where the C12 pendant group had a slightly depressed T_g of 75 °C compared to its C6 counterpart (79 °C). Moreover, T_{g_DMA} and T_{g_DSC} followed similar trends (Table 1).

To assess the effect of water uptake on thermomechanical properties, T_{g_sat} was measured after 40 days of water immersion to saturation. Nylon-6,6 showed the lowest T_{g_sat} in accordance with its high water uptake (Table 2, Figures S10-11), suffering an 80 °C depression from its dry value. The copolymers exhibited less plasticization with higher T_{g_sat} values, e.g., CH1DA-TD showed only a 54 °C reduction. Additionally, CH1DA-OC/TD exhibited a higher T_g than alternatives like Nylon-6,10, due to the difference in backbone rigidity in the polymers.[36] This demonstrates the performance advantages of novel cyclic monomers over a linear polyamide system.

To illustrate the platform nature of the DA-based derivatization of MA, we grafted allylbenzene (AB) to dm*tt*M. This aromatic pendant group was chosen to enhance char formation, a key metric toward inhibiting

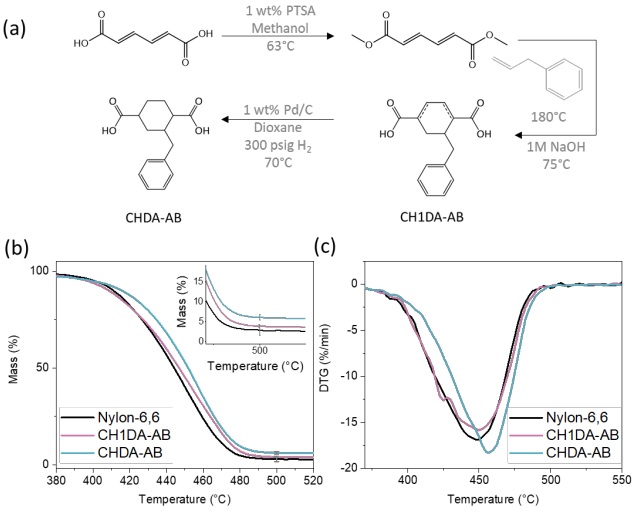

Figure 5. (a) DA-upgrading of ttMA with AB to generate char enhancing diacids. (b) TGA and (c) DTG (triplicate average) graphs of polyamides with 25 mol% loading of novel diacids.

flame spread.[37,38] Additionally, hydrogenation of the double bond (CHDA-AB) would further enhance thermal stability and also preclude any potential for retro-Diels-Alder under char-forming temperatures (Figures 5a, S12-S14, Table S4). A comparison of char yields between CH1DA-AB and CHDA-AB elucidated the role of the unsaturation in the design of flame-retardant monomers using the synthesis technique outlined here. TGA (triplicate runs) was carried out on each polyamide under an inert environment. From Figure 5b it is inferred that hydrogenated CHDA-AB (6.1% ± 0.61), with its aromatic pendant group, achieved a doubling in char with respect to neat Nylon-6,6 (2.9% ± 1.2). Interestingly, a difference in char yield was observed between CH1DA-AB (3.9% ± 0.36) and CHDA-AB. Inspection of the DTG curves (Figure 5c, Figure S8) showed an increase in T_{d10} by 7 °C for CHDA-AB, which together with the aromatic pendant serves to enhance char formation. Further increases in condensed-phase action to impede flammability can likely be achieved using vinyl-based phosphorus and nitrogen groups[39] using the DA-derivatization strategy.

This study illustrates the rapid differentiation of MA to novel monomers using the highly versatile DA reaction, facilitating the development of Nylon-6,6 copolymers with tailored properties. More broadly, the pairing of platform with diversity-oriented synthesis techniques presents an efficient strategy for developing performance-advantaged biopolymers. The adaptation of this approach to other platforms will accelerate the embrace of sustainable materials through the proliferation of new and useful plastics.

SUPPORTING INFORMATION

Experimental procedures for the synthesis of monomers and polymers, additional characterizations including ^{1}H and ^{13}C NMR, elemental analysis, GPC, DSC, TGA, WAXS, water uptake, contact angle, and rheology results.

ACKNOWLEDGMENTS

This material is based upon work supported by the U.S. Department of Energy's Office of Energy Efficiency and Renewable Energy (EERE) under the Bioenergy Technologies Office Award Number DE-EE0008492, and by the National Science Foundation under Award Number DMR-1626315. We thank Dr. Sarah Cady (ISU Chemical Instrumentation Facility) for training and assistance pertaining to the NMR and elemental analysis results included in this publication. We also thank the Keck Lab for their assistance with acquiring gass chromatography mass spectrometry results, Dr. Tracey Stewart for transmission electron microscopy imaging, Dustin Gansebom for helping with gel permeation chromatography analysis, Dr. Rui Li and AKM Mashud Alam (ISU Laboratories for Functional Textiles and Protective Clothing) for the contact angle pictures.

REFERENCES

(1) Iwata, T. Biodegradable and Bio-Based Polymers: Future Prospects of Eco-Friendly Plastics. *Angew. Chem. Int. Ed.* **2015**, *54* (11), 3210–3215. https://doi.org/10.1002/anie.201410770.

(2) Lu, R.; Lu, F.; Chen, J.; Yu, W.; Huang, Q.; Zhang, J.; Xu, J. Production of Diethyl Terephthalate from Biomass-Derived Muconic Acid. *Angew. Chem. Int. Ed.* **2016**, *55* (1), 249–253. https://doi.org/10.1002/anie.201509149.

(3) Deng, W.; Yan, L.; Wang, B.; Zhang, Q.; Song, H.; Wang, S.; Zhang, Q.; Wang, Y. Efficient Catalysts for the Green Synthesis of Adipic Acid from Biomass. *Angew. Chem. Int. Ed.* **2021**, *60* (9), 4712–4719. https://doi.org/10.1002/anie.202013843.

(4) Hočevar, B.; Prašnikar, A.; Huš, M.; Grilc, M.; Likozar, B. H_2 -Free Re-Based Catalytic Dehydroxylation of Aldaric Acid to Muconic and Adipic Acid Esters. *Angew. Chem. Int. Ed.* **2021**, *60* (3), 1244–1253. https://doi.org/10.1002/anie.202010035.

(5) Hernández, N.; Williams, R. C.; Cochran, E. W. The Battle for the "Green" Polymer. Different Approaches for Biopolymer Synthesis: Bioadvantaged vs. Bioreplacement. *Org. Biomol. Chem.* **2014**, *12* (18), 2834–2849. https://doi.org/10.1039/C3OB42339E.

(6) Suastegui, M.; Matthiesen, J. E.; Carraher, J. M.; Hernandez, N.; Rodriguez Quiroz, N.; Okerlund, A.; Cochran, E. W.; Shao, Z.; Tessonnier, J.-P. Combining Metabolic Engineering and Electrocatalysis: Application to the Production of Polyamides from Sugar. *Angew. Chem. Int. Ed.* **2016**, *55* (7), 2368–2373. https://doi.org/10.1002/anie.201509653.

(7) de Jong, E.; Dam, M. A.; Sipos, L.; Gruter, G.-J. M. Furandicarboxylic Acid (FDCA), A Versatile Building Block for a Very Interesting Class of Polyesters. In *ACS Symposium Series*; Smith, P. B., Gross, R. A., Eds.; American Chemical Society: Washington, DC, 2012; Vol. 1105, pp 1–13. https://doi.org/10.1021/bk-2012-1105.ch001.

(8) Stockmann, P. N.; Van Opdenbosch, D.; Poethig, A.; Pastoetter, D. L.; Hoehenberger, M.; Lessig, S.; Raab, J.; Woelbing, M.; Falcke, C.; Winnacker, M.; Zollfrank, C.; Strittmatter, H.; Sieber, V. Biobased Chiral Semi-Crystalline or Amorphous High-Performance Polyamides and Their Scalable Stereoselective Synthesis. *Nat Commun* **2020**, *11* (1), 509. https://doi.org/10.1038/s41467-020-14361-6.

(9) Winnacker, M.; Sag, J.; Tischner, A.; Rieger, B. Sustainable, Stereoregular, and Optically Active Polyamides via Cationic Polymerization of ε-Lactams Derived from the Terpene β-Pinene. *Macromol. Rapid Commun.* **2017**, *38* (9), 1600787. https://doi.org/10.1002/marc.201600787.

(10) Winnacker, M.; Sag, J. Sustainable Terpene-Based Polyamides *via* Anionic Polymerization of a Pinene-Derived Lactam. *Chem. Commun.* **2018**, *54* (7), 841–844. https://doi.org/10.1039/C7CC08266E.

(11) Shanks, B. H.; Broadbelt, L. J. A Robust Strategy for Sustainable Organic Chemicals Utilizing Bioprivileged Molecules. *ChemSusChem* **2019**, cssc.201900323. https://doi.org/10.1002/cssc.201900323.

(12) Shanks, B. H.; Keeling, P. L. Bioprivileged Molecules: Creating Value from Biomass. *Green Chem.* **2017**, *19* (14), 3177–3185. https://doi.org/10.1039/C7GC00296C.

(13) Khalil, I.; Quintens, G.; Junkers, T.; Dusselier, M. Muconic Acid Isomers as Platform Chemicals and Monomers in the Biobased Economy. *Green Chem.* **2020**, *22* (5), 1517–1541. https://doi.org/10.1039/C9GC04161C.

(14) Vardon, D. R.; Franden, M. A.; Johnson, C. W.; Karp, E. M.; Guarnieri, M. T.; Linger, J. G.; Salm, M. J.; Strathmann, T. J.; Beckham, G. T. Adipic Acid Production from Lignin. *Energy Environ. Sci.* **2015**, *8* (2), 617–628. https://doi.org/10.1039/C4EE03230F.

(15) Zhou, X.; Brentzel, Z. J.; Kraus, G. A.; Keeling, P. L.; Dumesic, J. A.; Shanks, B. H.; Broadbelt, L. J. Computational Framework for the Identification of Bioprivileged Molecules. *ACS Sustainable Chem. Eng.* **2019**, *7* (2), 2414–2428. https://doi.org/10.1021/acssuschemeng.8b05275.

(16) Vardon, D. R.; Rorrer, N. A.; Salvachúa, D.; Settle, A. E.; Johnson, C. W.; Menart, M. J.; Cleveland, N. S.; Ciesielski, P. N.; Steirer, K. X.; Dorgan, J. R.; Beckham, G. T. Cis,Cis-Muconic Acid: Separation and Catalysis to Bio-Adipic Acid for Nylon-6,6 Polymerization. *Green Chem.* **2016**, *18* (11), 3397–3413. https://doi.org/10.1039/C5GC02844B.

(17) Capelli, S.; Motta, D.; Evangelisti, C.; Dimitratos, N.; Prati, L.; Pirola, C.; Villa, A. Bio Adipic Acid Production from Sodium Muconate and Muconic Acid: A Comparison of Two Systems. *ChemCatChem* **2019**, *11* (13), 3075–3084. https://doi.org/10.1002/cctc.201900343.

(18) Collias, D. I.; Harris, A. M.; Nagpal, V.; Cottrell, I. W.; Schultheis, M. W. Biobased Terephthalic Acid Technologies: A Literature Review. *Industrial Biotechnology* **2014**, *10* (2), 91–105. https://doi.org/10.1089/ind.2014.0002.

(19) Carraher, J. M.; Pfennig, T.; Rao, R. G.; Shanks, B. H.; Tessonnier, J.-P. Cis,Cis-Muconic Acid Isomerization and Catalytic Conversion to Biobased Cyclic-C6 -1,4-Diacid Monomers. *Green Chem.* **2017**, *19* (13), 3042–3050. https://doi.org/10.1039/C7GC00658F.

(20) Rorrer, N. A.; Vardon, D. R.; Dorgan, J. R.; Gjersing, E. J.; Beckham, G. T. Biomass-Derived Monomers for Performance-Differentiated Fiber Reinforced Polymer Composites. *Green Chem.* **2017**, *19* (12), 2812–2825. https://doi.org/10.1039/C7GC00320J.

(21) Beerthuis, R.; Rothenberg, G.; Shiju, N. R. Catalytic Routes towards Acrylic Acid, Adipic Acid and ε-Caprolactam Starting from Biorenewables. *Green Chem.* **2015**, *17* (3), 1341–1361. https://doi.org/10.1039/C4GC02076F.

(22) Coudray, L.; Bui, V.; Frost, J. W.; Schweitzer, D. Process for Preparing Caprolactam and Polyamides Therefrom. 20130085255, April 4, 2013.

(23) Müller, C.; Bock, M.; SILVA, M. D.; Fischer, R.-H.; BLANK, B.; Kindler, A.; Melder, J.-P.; Otto, B.; SCHELWIES, M.; Henninger, A. Method for Producing Hexamethylenediamine. WO2015086819A1, June 18, 2015.

(24) Carraher, J. M.; Carter, P.; Rao, R. G.; Forrester, M. J.; Pfennig, T.; Shanks, B. H.; Cochran, E. W.; Tessonnier, J.-P. Solvent-Driven Isomerization of *Cis* , *Cis* -Muconic Acid for the Production of Specialty and Performance-Advantaged Cyclic Biobased Monomers. *Green Chem.* **2020**, *22* (19), 6444–6454. https://doi.org/10.1039/D0GC02108C.

(25) Dell'Anna, M. N.; Laureano, M.; Bateni, H.; Matthiesen, J. E.; Zaza, L.; Zembrzuski, M. P.; Paskach, T. J.; Tessonnier, J.-P. Electrochemical Hydrogenation of Bioprivileged *Cis* , *Cis* -Muconic Acid to *Trans* -3-Hexenedioic Acid: From Lab Synthesis to Bench-Scale Production and Beyond. *Green Chem.* **2021**, *23* (17), 6456–6468. https://doi.org/10.1039/D1GC02225C.

(26) Matthiesen, J. E.; Carraher, J. M.; Vasiliu, M.; Dixon, D. A.; Tessonnier, J.-P. Electrochemical Conversion of Muconic Acid to Biobased Diacid Monomers. *ACS Sustainable Chem. Eng.* **2016**, *4* (6), 3575–3585. https://doi.org/10.1021/acssuschemeng.6b00679.

(27) Settle, A. E.; Berstis, L.; Rorrer, N. A.; Roman-Leshkóv, Y.; Beckham, G. T.; Richards, R. M.; Vardon, D. R. Heterogeneous Diels–Alder Catalysis for Biomass-Derived Aromatic Compounds. *Green Chem.* **2017**, *19* (15), 3468–3492. https://doi.org/10.1039/C7GC00992E.

(28) Briou, B.; Améduri, B.; Boutevin, B. Trends in the Diels–Alder Reaction in Polymer Chemistry. *Chem. Soc. Rev.* **2021**, 10.1039.DoCS01382J. https://doi.org/10.1039/DoCS01382J.

(29) Stille, J. K. Step-Growth Polymerization. *J. Chem. Educ.* **1981**, *58* (11), 862. https://doi.org/10.1021/ed058p862.

(30) The Crystal Structures of Two Polyamides ('Nylons'). *Proc. R. Soc. Lond. A* **1947**, *189* (1016), 39–68. https://doi.org/10.1098/rspa.1947.0028.

(31) Abdolmohammadi, S.; Gansebom, D.; Goyal, S.; Lee, T.-H.; Kuehl, B.; Forrester, M. J.; Lin, F.-Y.; Hernández, N.; Shanks, B. H.; Tessonnier, J.-P.; Cochran, E. W. Analysis of the Amorphous and Interphase Influence of Comononomer Loading on Polymer Properties toward Forwarding Bioadvantaged Copolyamides. *Macromolecules* **2021**, *54* (17), 7910–7924. https://doi.org/10.1021/acs.macromol.1c00651.

(32) *Nylon Plastics Handbook*; Kohan, M. I., Ed.; Hanser Publishers ; Distributed in the USA and in Canada by Hanser/Gardner Publications: Munich ; New York : Cincinnati, 1995.

(33) Moran, C. S.; Barthelon, A.; Pearsall, A.; Mittal, V.; Dorgan, J. R. Biorenewable Blends of Polyamide-4,10 and Polyamide-6,10. *J of Applied Polymer Sci* **2016**, *133* (45), app.43626. https://doi.org/10.1002/app.43626.

(34) Palmer, R. J.; Updated by Staff. Polyamides, Plastics. In *Kirk-Othmer Encyclopedia of Chemical Technology*; John Wiley & Sons, Inc., Ed.; John Wiley & Sons, Inc.: Hoboken, NJ, USA, 2005; p 1612011916011213.a01.pub2. https://doi.org/10.1002/0471238961.1612011916011213.a01.pub2.

(35) Guidotti, G.; Soccio, M.; Siracusa, V.; Gazzano, M.; Munari, A.; Lotti, N. Novel Random Copolymers of Poly(Butylene 1,4-Cyclohexane Dicarboxylate) with Outstanding Barrier Properties for Green and Sustainable Packaging: Content and Length of Aliphatic Side Chains as Efficient Tools to Tailor the Material's Final Performance. *Polymers* **2018**, *10* (8), 866. https://doi.org/10.3390/polym10080866.

(36) Greco, R.; Nicolais, L. Glass Transition Temperature in Nylons. *Polymer* **1976**, *17* (12), 1049–1053. https://doi.org/10.1016/0032-3861(76)90005-7.

(37) van Krevelen, D. W. Some Basic Aspects of Flame Resistance of Polymeric Materials. *Polymer* **1975**, *16* (8), 615–620. https://doi.org/10.1016/0032-3861(75)90157-3.

(38) Velencoso, M. M.; Battig, A.; Markwart, J. C.; Schartel, B.; Wurm, F. R. Molecular Firefighting-How Modern Phosphorus Chemistry Can Help Solve the Challenge of Flame Retardancy. *Angew. Chem. Int. Ed.* **2018**, *57* (33), 10450–10467. https://doi.org/10.1002/anie.201711735.

(39) Braun, U.; Schartel, B.; Fichera, M. A.; Jäger, C. Flame Retardancy Mechanisms of Aluminium Phosphinate in Combination with Melamine Polyphosphate and Zinc Borate in Glass-Fibre Reinforced Polyamide 6,6. *Polymer Degradation and Stability* **2007**, *92* (8), 1528–1545. https://doi.org/10.1016/j.polymdegradstab.2007.05.007.

Table of Content artwork